File

FILE COPY

O T T A W A November 15th, 1944.

R E P O R T

of the

ORE DRESSING AND METALLURGICAL LABORATORIES.

Investigation No. 1715.

Armour Plate Cooling Rates in Welding.
PART II. - Unionmelt Automatic Welding.

(Note: Part I, on manual welding, was issued on October 2nd, 1944.)

(Copy No. 10 .)

O T T A W A November 15th, 1944.

R E P O R T

of the

ORE DRESSING AND METALLURGICAL LABORATORIES.

Investigation No. 1715.

Armour Plate Cooling Rates in Welding.
PART II. - Unionmelt Automatic Welding.

Introduction:

This part of the present investigation is specifically concerned with Unionmelt automatic welding and the resultant cooling rates in the heat-affected zones. As in Part 1, it was desired to determine the cooling rates associated with normal welding practice and the variations of these cooling rates that could be obtained by varying welding conditions within practical limits. The transformation products resulting from these varying cooling rates are of prime importance and are a function of the time-temperature relations above the equilibrium temperature.

This investigation is concerned with the effects of welding conditions on the base metal of the heat-affected zones and is limited to certain areas within the zones as determined by thermocouple location.

Material:

The material used was standard bulletproof plate, 12 mm. in thickness, made by the Dominion Foundries and Steel Limited, Hamilton, Ontario. This steel is made to the following specification:

	Per Cent		Per Cent
Carbon -	0.20-0.30	Chromium -	0.80-1.10
Manganese -	0.70-0.90	Nickel -	0.70-0.90
Silicon -	0.40-0.60	Molybdenum -	0.20-0.30

One large plate was used, being cut into sections 12 in. x 36 in. Unfortunately, it was impossible to obtain the heat or plate number. A chemical analysis of this plate gave the following results:

	Per Cent		Per Cent
Carbon -	0.24	Chromium -	0.94
Manganese -	0.78	Nickel -	0.70
Silicon -	0.54	Molybdenum -	0.20

Equipment:

All welds were made with the Unionmelt Type "U" welding head operating on A.C. current, No. 80 melt of 12 x 200 sizing and No. 40 3/16-in. diameter Dominion Oxygen Co. electrode. This electrode deposits metal of the following analysis:

	Per Cent		Per Cent
Carbon -	0.14-0.17	Chromium -	Trace.
Manganese -	1.8-2.20	Nickel -	Trace.
Silicon -	0.02	Molybdenum -	0.43-0.48

Welding currents were measured by inserting a Weston D.C. A.C. ammeter into the primary circuit of the welding transformer and multiplying the figures obtained by the appropriate factor. Open circuit and arc voltages were measured by connecting a Weston A.C. voltmeter between the welding head and the

(Equipment, cont'd) -

ground clamp.

Plate Preparation:

Plates were prepared by machine bevelling to a 45-degree included angle and a 1/16-in. root face. Plate sizes were 12 in. x 36 in., so that when a weld was completed a test plate 24 in. x 36 in. was secured. The plates were positioned in a jig used in armoured vehicle production and backed up with a copper bar 1 in. x 3 in. x 38 in. (Sketch No. 1). No preheat was used in any case. The temperature of the plates at beginning of welding was approximately 60° F.

Temperature Measurements:

Exactly the same system of temperature measurement was used as in Part I of this report. Here again temperatures were measured in a plane midway between the two surfaces of the plate and at various distances from the weld. Due to this selection of thermocouple location it should be emphasized that in the remainder of this report all remarks apply, unless otherwise indicated, only to the steel within this area. Holes were drilled in the plates to a depth of 6 mm. with a No. 51 drill. This size of hole is necessary to accommodate the thermocouple wire and its porcelain insulator and is too small to have more than a second order effect on heat flow. Each wire was welded onto the plate in separate holes, the centres of which were 1/8 in. apart, by the electrical discharge method[1]. Each weld was then tested, by a sharp pull, for mechanical soundness.

The characteristic current and voltage oscillations at the start of a Uniormelt weld necessitated location of thermocouples at least 1 foot from the starting end of a weld. Three sets of thermocouples were evenly spread over the

(Temperature Measurements, cont'd) -

remaining two feet in order to minimize the possibility of failure to secure a cooling rate recording because of thermocouple failure.

Procedure:

All welds were made in one pass and the speed of welding, energy input, etc., were recorded. Thermocouples were welded into position (Sketch No. 2) and the cooling rate obtained for each weld.

The energy input of each weld was calculated from the formula

$$\frac{\text{arc voltage x arc current x 60}}{\text{welding speed in inches per minute}} = \text{joules per inch energy input.}$$

Cooling rates, energy input, etc., were determined for three types of welds. These were those of high, low and normal energy input. The low-energy-input weld was made by employing the lowest arc energy possible consistent with good welding action. This limitation was established to remain within practical welding conditions. This same idea was carried forward to the high-energy-input weld. In the case of the normal-energy-input-weld, the welding conditions were those used in similar joints and thickness of plate in armoured vehicle production.

These cooling rates having been obtained, the TTT curve and Grange & Kiefer continuous cooling diagram used in Part I of this report could be employed to attempt to correlate cooling rates with the microstructures produced. While the analyses of the two plates used in both parts of this report are not identical their differences are not marked. Figure 1 shows the "transformation begins" line of both the TTT curve and the Grange &

(Procedure, cont'd) -

Kiefer cooling diagram of the steel used in the first part of this report. In subsequent charts these lines have been superimposed on the cooling curves obtained.

Data Obtained:

(1) Low-Energy-Input Weld -

Rod size, (diameter in inches)	Volts	Amps.	Welding speed, in./min.	Energy input, joules/inch	Maximum temperature recorded, ° F.
3/16	30	1,050	20	94,450	1680

Figure 2 shows the cooling rate obtained. Figure 3 shows a macrophotograph of a section of this weld through the centre of one of the thermocouple holes. It will be noted that the end of the hole is well within the heat-affected zone of the weld. Figure 4 shows the resultant microstructure produced at the end of the thermocouple hole. The Vickers hardness at this location was found to be 401.

(2) Normal-Energy-Input Weld -

Rod size, (diameter in inches)	Volts	Amps.	Welding speed, in./min.	Energy input, joules/inch	Maximum temperature recorded, ° F.
3/16	27	810	10	131,000	1910° F.

Figure 2 shows the cooling rate obtained. Figure 5 shows a macrophotograph of a section of this weld through the centre of one of the thermocouple holes. It will be noted that the end of the thermocouple hole is well within the heat-affected zone of the weld. Figure 6 shows the resultant microstructure produced at the end of the thermocouple hole. The Vickers hardness at this location was found to be 306.

(Continued on next page)

(Procedure, cont'd) -

(3) High-Energy-Input Weld -

Rod size, (diameter in inches)	Volts	Amps.	Welding speed, in./min.	Energy input, joules/inch	Maximum temperature recorded, ° F.
5/16	30	750	8	168,750	1605° F.

Figure 2 shows the cooling rate obtained. Figure 7 shows a macrophotograph of a section of this weld through one of the thermocouple holes. It will be noted that the end of the thermocouple hole is well within the heat-affected zone of the weld. Figure 8 shows the resultant microstructure produced at the end of the thermocouple hole. The Vickers hardness at this location was found to be 354.

Figure 9 shows the structure of the armour plate prior to welding. The Vickers hardness of the plate in this condition was found to be 327-342.

General Discussion:

In Part I of this report it was pointed out that the interpretation of austenitizing conditions and austenite transformation was subject to many difficulties. However, simplifications can be made which are restricted to certain particular cases. The cooling rates over almost the entire width of the heat-affected zone are roughly the same, which permits further simplification since only one thermocouple need be used and its location within the heat-affected zone is not critical. This conclusion was reached after recording simultaneously in the same heat-affected zone the time-temperature cycles with thermocouples located at varying distances from the fusion line. However, slight variations probably occur.

Factors influencing the austenite hardenability within the heat-affected zone are of prime importance. Consider first

(General Discussion, cont'd) -

the grain size. In the present case, the grain size effect is believed to be unimportant since evidence was obtained that the grain-coarsening temperature was higher than 2000° F. Because of the latent heat of solidification of steel the cooling rate is lowered in the region of higher temperatures and the increase in hardenability due to grain coarsening is more than compensated. It is common experience that the hardness of the region of the heat-affected zone close to the fusion line is lower than in the opposite direction although the steel is at its maximum hardenability. With respect to carbide inhomogeneities, they are also in this case believed to be of minor importance. This conclusion has been reached because of the fact that with equal cooling rates and grain sizes the hardnesses of the transformation products over the entire width of the heat-affected zone were almost equal. This means that the TTT curve is shifted insignificantly in the range where transformation occurs. This conclusion, however, must not be generalized, because there are many known cases where, in fact, hardness variations exist in the heat-affected zone and have to be explained in terms of the carbide inhomogeneities due to the equality of cooling rates and austenite grain size.

Thus we have reached the general conclusion that, in this particular case, difference in cooling rates is the chief factor accounting for the hardness and ductility in the heat-affected zone.

It will be noted that in all macrophotographs the width of the heat-affected zone is not the same on both sides of the weld. Hardness surveys reveal that in the case of the normal-energy-input weld the hardnesses on the side in which

(General Discussion, cont'd) -

the thermocouple was located were uniformly approximately 300 Vickers whereas on the opposite side hardnesses of 400 Vickers were recorded. This feature is very important, as it might invalidate results of investigations made only on one side of a weld. The differences in widths of the heat-affected zones and the differences in hardness of these zones indicate a considerable difference in energy distribution and absorption and consequently varying cooling rates. In effect, measurements made on the low-energy welds have been made on what might be described as the low-energy side of the low-energy weld. This is believed to be due to imperfect alignment of the welding head with the centre line of the joint.

(1) Low-Energy-Input Weld -

The resultant microstructure at the end of the thermocouple hole was found to be fine-grained, acicular, and uniform. The hardness obtained and the structure in this area are in agreement with the cooling rate obtained and its relation to the Grange & Kiefer cooling diagram. It will be noted from Figure 2 that the cooling curve intersects the Grange & Kiefer cooling diagram in the bainite range and that the cooling curve is relatively steep, which implies incomplete transformation to bainite when the M point is reached. Consequently a structure a composite of bainite and martensite would be expected, and, as shown by Figure 4, has been produced.

The uniformity of the structure, while not evidence of absence of segregation, shows that at least the transformation products are uniform within themselves. In Figure 3 (macrophotograph), note the marked difference in the width of the heat-affected zone on the two sides of the weld.

The length of time at the austenitizing temperature

(General Discussion, cont'd) -

(9.2 seconds at above the Ac_3 temperature) would probably not be sufficient to produce homogeneous austenite, so that displacement of the TTT curve, and consequently the cooling diagram, towards shorter times, is inevitable. This shift is believed to be of minor importance.

(2) Normal- and High-Energy-Input Welds -

The microstructures at the ends of the thermocouple holes (shown in Figures 6 and 8) are fairly characteristic of those found within these areas. However, considerable variation in structure was noted within this area. Hardness surveys made across the heat-affected zones have shown uniform hardness at least along that side on which the thermocouple was located. Two different thermocouples (different distances from the fusion line) gave almost exactly the same cooling rates in the case of both welds although the maximum temperatures attained were different. For the normal-energy-input weld the two thermocouples recorded maximum temperatures of 1910° F. and 2000° F. and in the high-energy-input weld 1605° F. and 2200° F. From the cooling curves obtained in each case it can be concluded that the cooling rates are almost independent of the maximum temperature attained. The hardness surveys in each case have not shown any significant difference which, in turn, indicates independence of the maximum temperature attained. This would indicate that in this case the displacement of the TTT curve due to differences of carbide inhomogeneities (it would be expected that better carbide solution would occur at the higher temperatures) encountered in the varying austenitizing conditions is negligible. Briefly, the cooling rate appears to be the sole important factor.

In order to relate the cooling rate to the transformation products on cooling, only the cooling rate in the region

(General Discussion, cont'd) -

where transformation actually occurs should be considered for all practical purposes. The differences in hardness between the two welds appear to be inexplicable on the basis of the resultant microstructures. On the other hand, on the basis of Grossman's criterion of hardenability of half temperature times (half temperature times between the maximum temperature and room temperature) the hardness of the normal-energy-input weld should be higher than that of the high-energy-input weld. However, the fact that these calculations allow for time spent above the A_e temperatures is n o t theoretically sound, since transformations take place at considerably lower temperatures.

An explanation was achieved by considering the cooling rates in the region of the bainite-martensite range - that is, from 1000° F. to 500° F. In this range the high-energy-input weld shows a steeper slope than the normal-energy-input weld although the times from the lower A_e temperature to 500° F. are the same. The mechanics of transformation at this time are still being debated. One would expect that faster cooling rates would lead to harder transformation products.

In both structures banding was found and this is an evidence of segregation in austenite. From the standpoint of transformation of the austenite, banding will show up according to the differences in carbon and alloy contents of the bands and also to variations in cooling rates. It is known, for example, that carbon has a much more pronounced effect on the displacement of the M point than the common alloying elements (Ni, Mn, Cr, etc.). On the other hand these alloying elements will displace the nose of the TTT curve more than will carbon. According to the relative displacement of certain regions of the TTT curve and the cooling rates involved, segregation will show

(General Discussion, cont'd) -

or will not show in the microstructure. For example, the microstructure of a fully quenched steel containing segregation of alloying elements will not show segregation, whereas the same steel will show bands in the annealed condition. This is because the M point of the segregated regions is but slightly displaced but the top region of the TTT curve is more drastically affected.

Banding introduces one more complexity into the problem of interpretation because the hardness of the resultant microstructure is a resultant of two components of differing individual hardnesses the exact proportions of which are unknown. Within one heat of steel, segregation would be the same if the melting and rolling practices are the same. In addition, segregation has a different importance, according to the cooling rates involved, as explained above. In this case, on the basis of microstructure and cooling rates the consequences of segregation are believed to be of the same order in both the normal and the high-energy-input welds.

CONCLUSIONS:

1. Under the conditions of this investigation the cooling rates at the centre of a 12-mm. plate of a single-pass automatic weld may be varied from averages of 8.3 to 4.75 Fahrenheit degrees per second between the lower critical and the Ar'' range. This variation of cooling rates is obtained by varying the energy input of the weld. It should be emphasized that these average cooling rates were obtained on what might be termed the low-energy side of the welds.

2. The most important single factor determining the hardness and ductility of the heat-affected zone is the cooling

(Conclusions, cont'd) -

rate through the important subcritical temperature ranges.

3. In this investigation it has been shown that measurement of cooling rates within the heat-affected zone is possible but that the correlation of cooling rates with the cooling diagram is impossible due to pronounced banding of the steel.

4. Cooling rates are essentially the same over the entire width of the heat-affected zone and are independent of the maximum temperature attained.

5. The use of hardness surveys on one side of a weld, as a means of prediction of the ductility of the joint, is of doubtful value. Slight misalignment of the welding head with the centre line of the joint results in concentration of heat towards one side of the weld and a consequent variation in hardness between the two sides.

Commentary:

It must be conceded that the prime objective of this investigation has not been attained. However, some trends are noticeable and worthy of comment.

The thermal cycle of welding of low-energy-input welds is such as to produce a hard, fine microstructure. The fact that this thermal cycle was determined on the low-energy side of the low-energy weld does not alter this statement. In other words, the hardenability of the plate has been used to good effect. This characteristic might prove useful in welding of low hardenability heats.

The effects of the thermal cycles of welding with the normal and high-energy-input techniques are more difficult to assess. It would appear that the best use of these techniques

(Commentary, cont'd) -

would be confined to high hardenability armour plate in which excess hardening is to be avoided.

It should be noted that these trends are the direct opposite of those noted in the manual welding part of this investigation.

Acknowledgements:

It is a pleasure to acknowledge the co-operation of Mr. J. A. Rice, Superintendent and Vice-President of the International Harvester Company, Hamilton, Ontario. The field work of this investigation was conducted at the above company's plant, with the full co-operation of the staff.

Reference.

(1) The Welding Journal, Sept. 1943, p. 383s.

oooooooooo
oooooo
oo

HJN:GHB.

ADDENDUM

In both Part I and Part II of this report, grain size and austenite inhomogeneity factors have been such as to prevent correlation of cooling rates with microstructures.

The welding of high hardenability materials produces within the heat-affected zone a hard, coarse-grained structure. This structure is associated with high maximum temperatures and possible complete solution of carbides and alloys in the austenite. The cooling rate, if just exceeding the critical cooling rate, will result in the maximum hardenability of the steel being developed in these areas. The response of the remainder of the heat-affected zones to the cooling rate is conditioned upon the smaller grain size and lower maximum temperatures obtained, with consequent inhomogeneity of the austenite. The result would be a lower development of the potential hardenability and probably superior ballistic performance. In brief, in the case of the high hardenability materials the hard, coarse-grained area is least able to resist shock and penetration and is therefore critical.

In the welding of lower hardenability materials the development of maximum hardenability in the coarse-grained area of the heat-affected zone would not be expected to produce the same sensitivity to shock and penetration as in the high hardenability materials. The weakest area within the heat-affected zone would be that in which the grain size is fine and the maximum temperature attained relatively low with the consequent inhomogeneity of austenite. Here the maximum hardenability is not developed and this, in conjunction with low potential hardenability, presumably would result in low resistance to penetration.

Materials of medium hardenability are more difficult to assess in regard to their response to the thermal cycle of

(Addendum, cont'd) -

welding. At the moment it is not known where the dividing line between high and low hardenability should be drawn. It is quite probable that both of the areas discussed above would be critical.

Now that some knowledge of the thermal cycle of welding has been obtained, attempts to duplicate these cycles could be made by heat-treating methods. If this is possible with very small samples, it might also be possible to develop a modified TTT curve and a Grange & Kiefer type cooling diagram which would permit accurate prediction of resultant microstructures associated with the cooling rates available. This method would, of course, consider grain size and austenite inhomogeneity factors as a part of the modified TTT curve. Consideration has been given to the measurement of inhomogeneity in austenite and one particular method shows promise.

The undertaking of additional research is under consideration. In the event that it is decided to extend this work and results of interest and importance are secured, an additional report will be issued.

HJN:GHB.

SKETCH NO. 1.

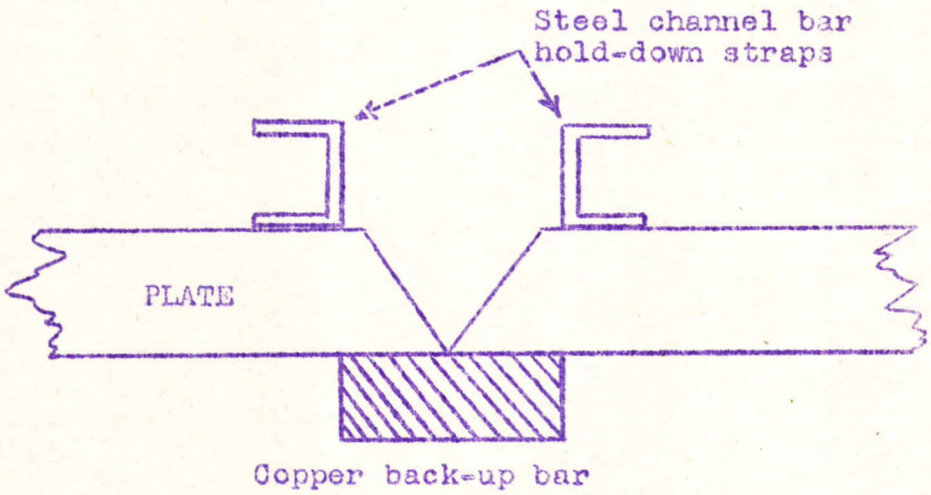

SKETCH NO. 2.

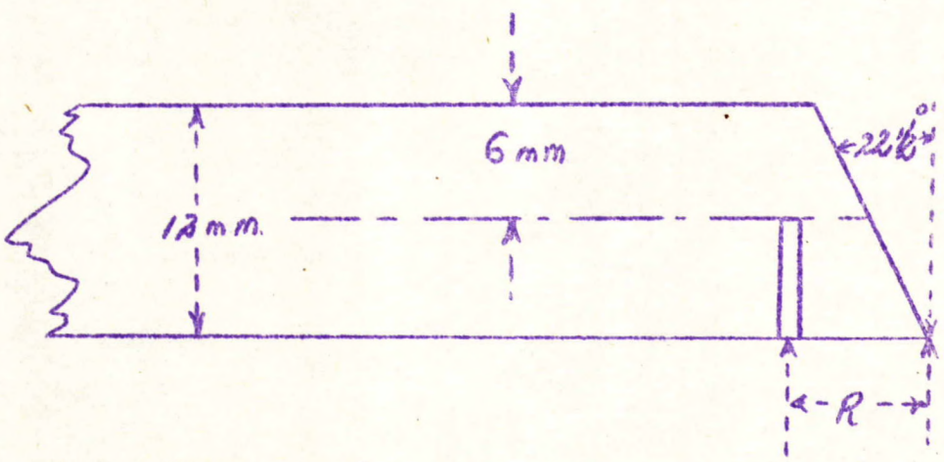

R = Distance of centre of thermocouple hole from bottom edge of plate.

R varied with heat input of weld. End of thermocouple always within the heat-affected zone of weld. Necessary length of R determined by trial and error.

GRANGE AND KIEFFER COOLING DIAGRAM AS DERIVED FROM THE S-CURVE.

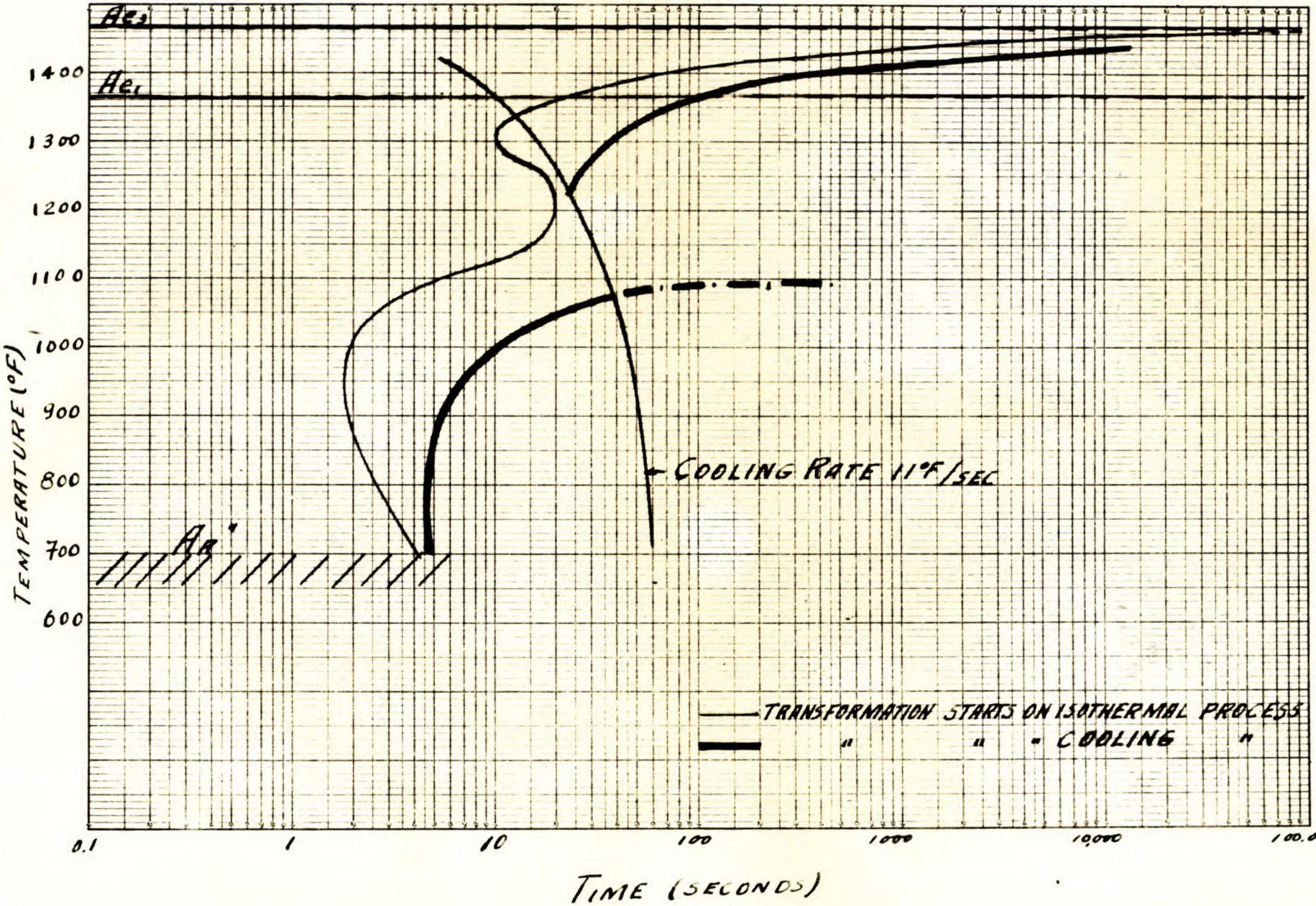

FIGURE 1.

Unionmelt Welding
Low and Normal Heat Input

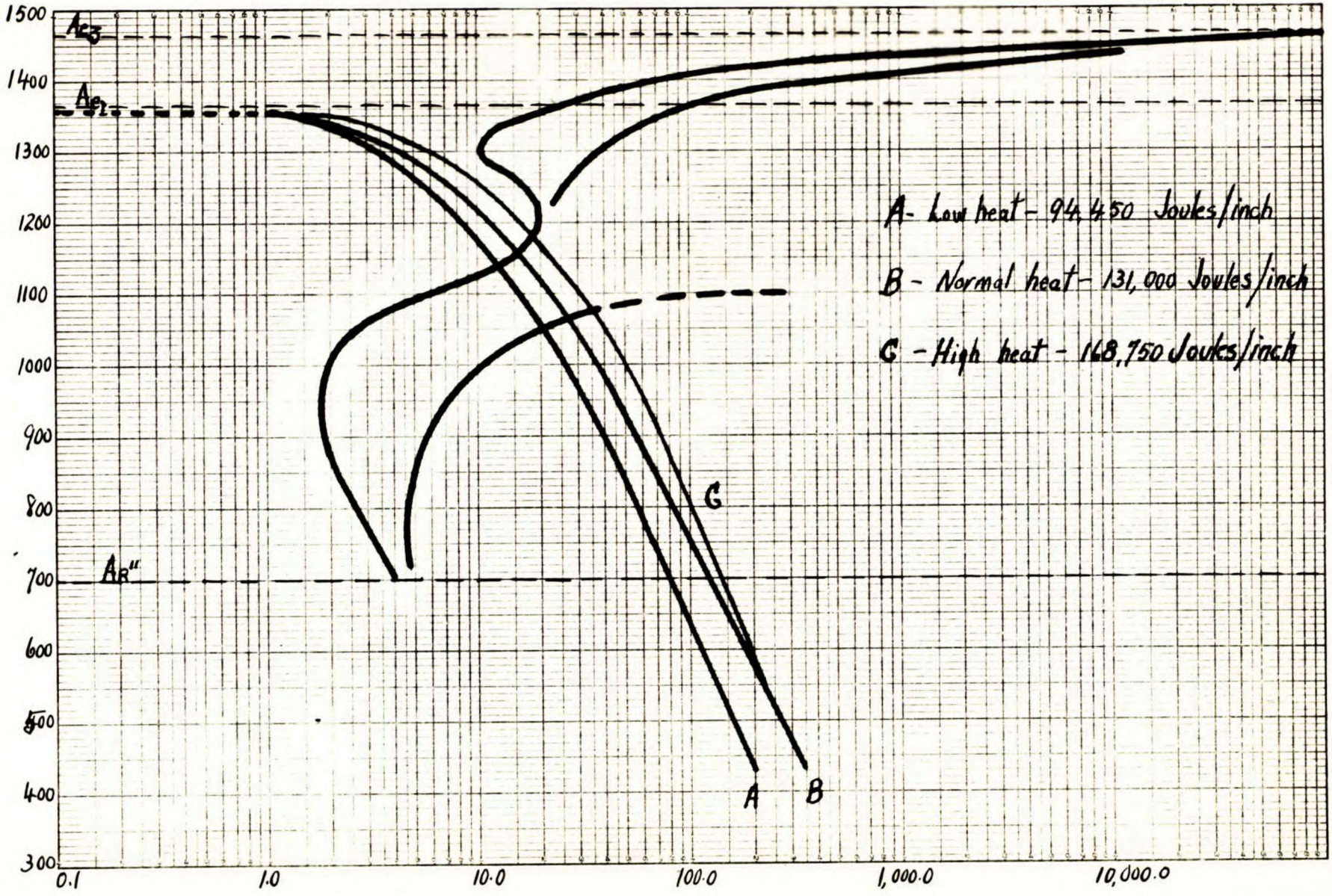

Figure 2.

Figure 3.

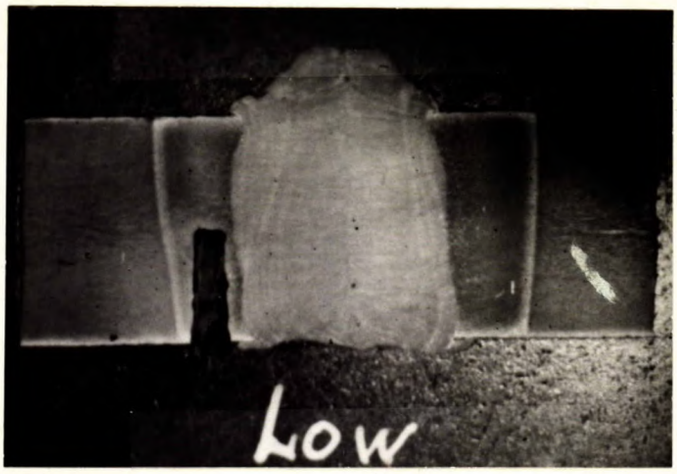

MACROPHOTOGRAPH OF WELD SECTION -
LOW-ENERGY INPUT.

Note end of thermocouple hole well within the heat-affected zone. Note, also, differences in width of heat-affected zone at two sides of weld.

—

Figure 4.

X500, etched in 4 per cent picric acid, 1 per cent HCl in alcohol.

RESULTANT STRUCTURE OF LOW-ENERGY-INPUT WELD.

Composite of martensite and bainite.
Note uniformity and fineness of structure.

—

Figure 5.

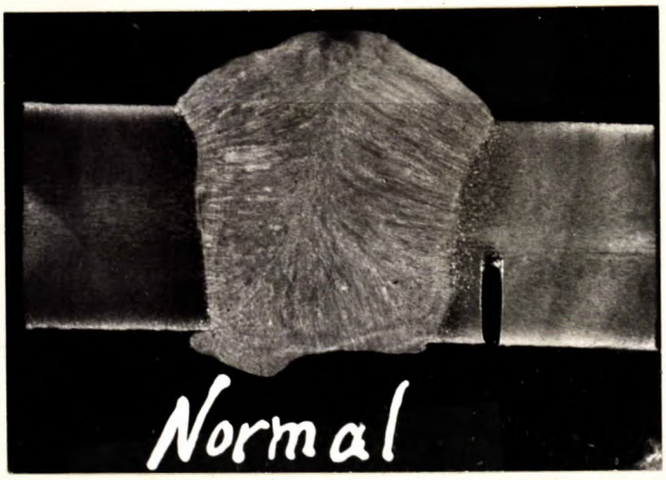

MACROPHOTOGRAPH OF SECTION OF NORMAL-ENERGY-INPUT WELD.

Note end of thermocouple hole well within the heat-affected zone. Note, also, the differences in width of heat-affected zone on the two sides of weld.

—

Figure 6.

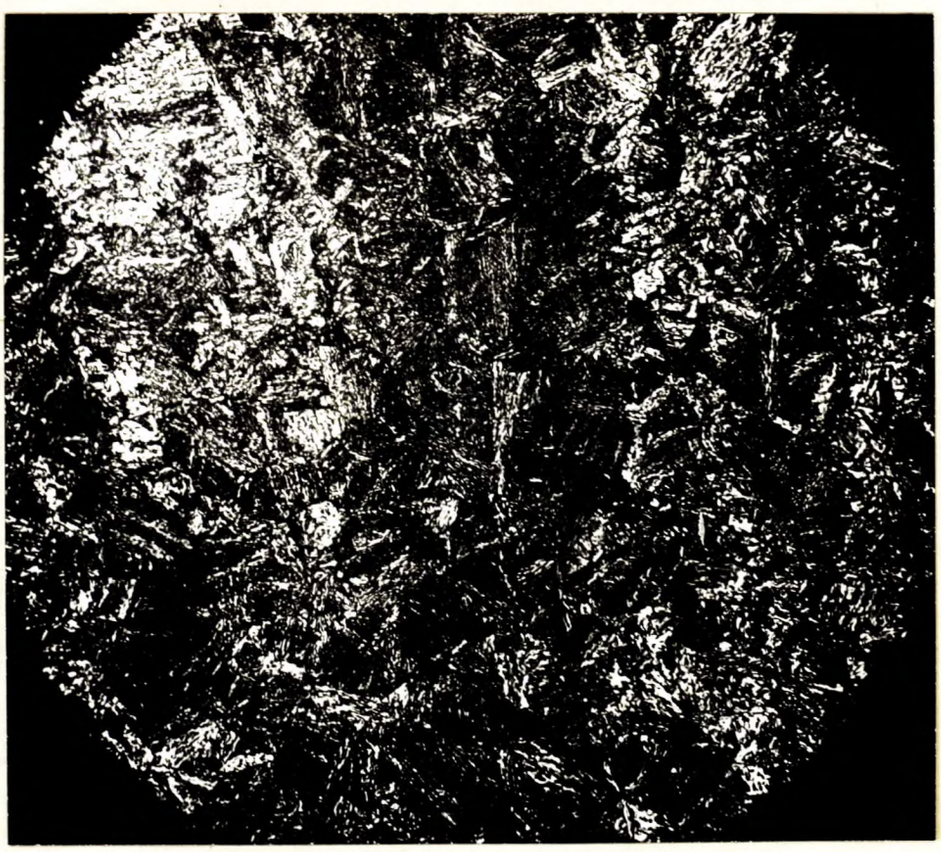

X500, etched in 4 per cent picric acid, 1 per cent HCl in alcohol.

RESULTANT STRUCTURE OF NORMAL-ENERGY-INPUT WELD.

Note differences of transformation products as a result of banding.

—

Figure 7.

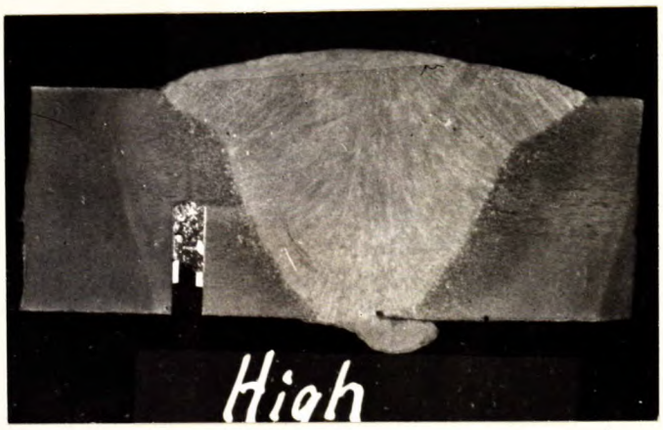

MACROPHOTOGRAPH OF SECTION OF HIGH-ENERGY-INPUT WELD.

Note end of thermocouple hole well within the heat-affected zone. Note, also, the differences in width of heat-affected zone on the two sides of weld.

—

Figure 8.

X500, etched in 4 per cent picric acid, 1 per cent HCl in alcohol.

RESULTANT STRUCTURE OF HIGH-ENERGY-INPUT WELD.

Note differences of transformation products as a result of banding.

—

Figure 9.

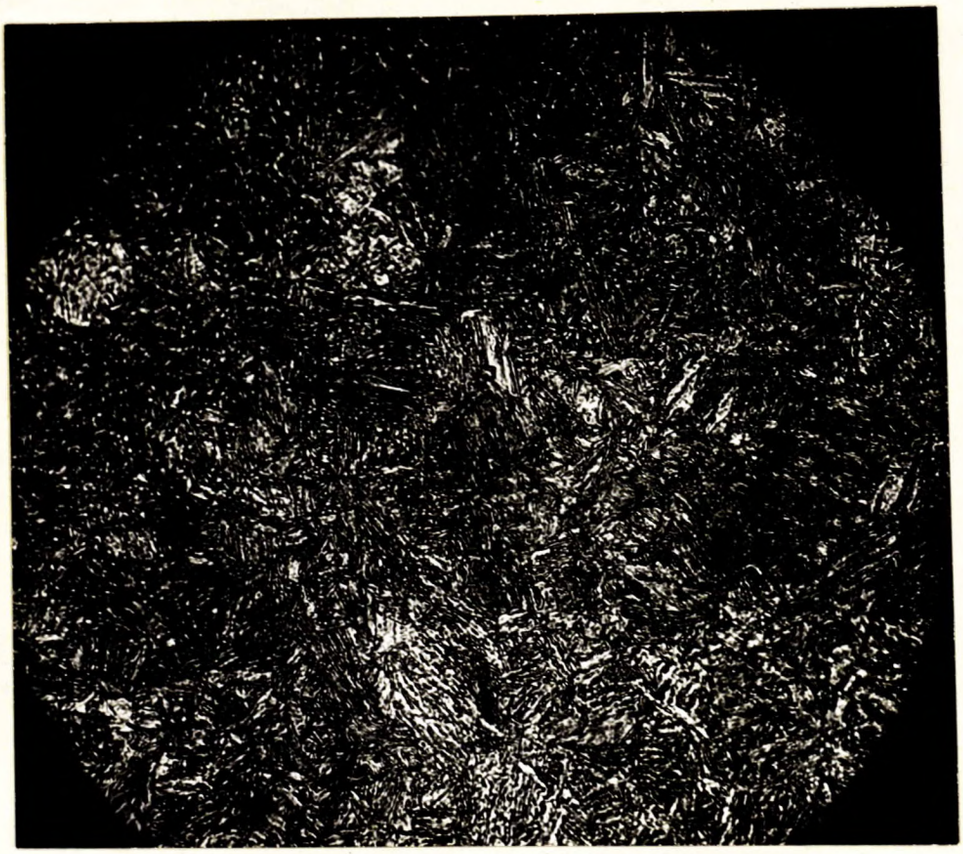

X500, etched in 4 per cent picric acid,
1 per cent HCl in alcohol.

NORMAL STRUCTURE OF ARMOUR PLATE.

H.J.N:G.H.B.